

Energy-Time-Accuracy Tradeoffs in Thermodynamic Computing

Alberto Rolandi,^{1,2} Paolo Abiuso,² Patryk Lipka-Bartosik,^{3,4}
Maxwell Aifer,⁵ Patrick J. Coles,^{5,*} and Martí Perarnau-Llobet^{6,†}

¹ Atominstitut, TU Wien, 1020 Vienna, Austria

² Institute for Quantum Optics and Quantum Information - IQOQI Vienna,
Austrian Academy of Sciences, Boltzmanngasse 3, A-1090 Vienna, Austria

³ Center for Theoretical Physics, Polish Academy of Sciences, Warsaw, Poland

⁴ Institute of Theoretical Physics, Jagiellonian University, 30-348 Kraków, Poland

⁵ Normal Computing Corporation, New York, New York, USA

⁶ Física Teòrica: Informació i Fenòmens Quàntics, Departament de Física,
Universitat Autònoma de Barcelona, 08193 Bellaterra (Barcelona), Spain

In the paradigm of thermodynamic computing, instead of behaving deterministically, hardware undergoes a stochastic process in order to sample from a distribution of interest. While it has been hypothesized that thermodynamic computers may achieve better energy efficiency and performance, a theoretical characterization of the resource cost of thermodynamic computations is still lacking. Here, we analyze the fundamental trade-offs between computational accuracy, energy dissipation, and time in thermodynamic computing. Using geometric bounds on entropy production, we derive general limits on the energy–delay–deficiency product (EDDP), a stochastic generalization of the traditional energy–delay product (EDP). While these limits can in principle be saturated, the corresponding optimal driving protocols require full knowledge of the final equilibrium distribution, i.e., the solution itself. To overcome this limitation, we develop quasi-optimal control schemes that require no prior information of the solution and demonstrate their performance for matrix inversion in overdamped quadratic systems. The derived bounds extend beyond this setting to more general potentials, being directly relevant to recent proposals based on non-equilibrium Langevin dynamics.

I. Introduction

Computational time, accuracy, and system size have long guided progress in computational architectures, algorithms, and hardware. With the rapid expansion of AI technologies, however, power consumption is becoming a central bottleneck in modern computing devices. A basic metric to quantify the balance between power and computational speed is the energy–delay product (EDP), defined as the product of the energy consumed and the execution time of a computation [1]. Clarifying the fundamental limits of EDP is crucial not only for optimizing current platforms, but also for assessing new physics-based approaches [2], such as thermodynamic computing [3, 4], which aims to exploit physical principles to achieve ultra-low-energy computation.

The limits of EDP go back to Landauer’s principle, which establishes a minimum energy cost for irreversible computations. Specifically, erasing one bit of information dissipates at least $k_B T \ln(2)$ Joules, where k_B is the Boltzmann constant and T is the system temperature [5]. Real implementations have substantial overheads, such as the energetic cost of precise timing control [6] and voltage switching [7], leakage currents arising due to scaling [8], or the cost of error data-memory movements [9]. Together, these contributions typically raise energy costs of computation by many orders of magnitude above the Landauer value. Even in the absence of such practical

limitations, achieving Landauer’s limit requires the system to remain in equilibrium at all times, so any (ideal) computation performed in finite time will necessarily lie above Landauer’s limit. To address this gap, recent advances in stochastic thermodynamics [10–12] have introduced finite-time extensions of Landauer’s bound [13–16] and characterized the energetics of minimal models of logic gates [17–24], both revealing that faster computations (i.e. shorter delays) entail higher energy costs. Furthermore, proof-of-principle experimental demonstrations of Landauer’s principle in colloidal particles, nanomagnetic systems and quantum molecular magnets, have been achieved [25–30].

Recent advances have further characterized EDP across diverse platforms. Progress on computational architectures, particularly CMOS-based systems, has shown that scaling transistor sizes and optimizing micro-architectures (e.g., variable pipeline depth) can modulate the EDP within physical constraints [31]. Meanwhile, emerging technologies like reversible computing, spintronics, and neuromorphic systems promise to push EDP closer to fundamental limits by minimizing or circumventing the energy cost of bit erasure [32], encoding information in low-energy states [33], and eliminating costly data movements [34]. However, practical challenges—such as noise, interconnect overheads, and thermal management—continue to separate theoretical bounds from achievable performance.

Thermodynamic computing is a leading candidate to accelerate AI workloads, from Bayesian inference to generative AI [3, 4, 35–39]. Moreover, it provides a clear opportunity for exploring energy-time tradeoffs and funda-

* patrick@normalcomputing.ai

† marti.perarnau@uab.cat

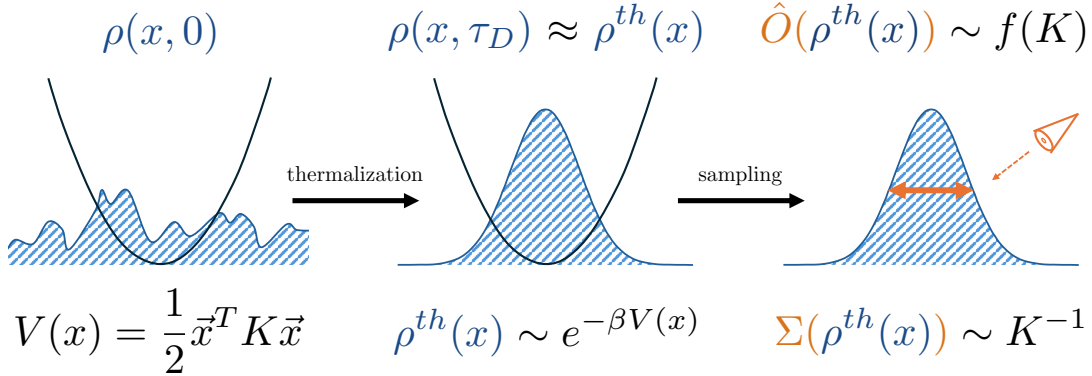


FIG. 1. **Thermodynamic algorithm for computing $f(K)$.** In this illustration, the probability density of the state (in blue) is in some arbitrary initial distribution when the potential $V(x) = \frac{1}{2} \vec{x}^T K \vec{x}$ (in black) is applied. The probability density of the state naturally evolves towards thermal equilibrium (Step 1), after which the observer can start sampling properties of the system to directly measure $f(K)$ (Step 2). For example, the correlation matrix Σ of the positions in the thermal distribution corresponds to the inverse of K .

mental bounds on the EDP. Thermodynamic computing algorithms have been developed for matrix inversion and linear systems [40], matrix exponentials [41], Bayesian inference [42], quadratic programming [43], and second-order optimization [44]. These algorithms typically involve a key step, which is a quench followed by a relaxation to thermal equilibrium. This protocol is, however, suboptimal in terms of EDP, and recent results suggest that alternative driving protocols can considerably reduce the energetic cost [45–48], potentially reaching the limits of the EDP.

Within this context, in this work we derive fundamental bounds on the EDP of thermodynamic computers and construct driving protocols that can approach them under realistic assumptions. We focus on quadratic potentials and equilibrium-based protocols [46], such as those in Gaussian sampling and linear algebra applications, although our results naturally extend to arbitrary potentials and out-of-equilibrium computations, including recent proposals for non-equilibrium thermodynamic computing [36, 49].

The paper is structured as follows. First, in Sec. II, we introduce a key quantity in our work, a natural extension of the EDP that explicitly incorporates the probabilistic nature of thermodynamic computation. The resulting energy–delay–deficiency product (EDDP) combines energy, time and reliability into a single metric for thermodynamic algorithms. In Sec. III, we characterize the EDDP of a driving protocol and derive a fundamental lower bound on it by leveraging the geometric concept of Wasserstein geodesic [50, 51]. In Sec. IV, we construct realistic driving protocols that can approach such bounds, and apply them to the problem of solving linear systems. Finally, we discuss extensions in Sec. V, and conclude in Sec. VI.

II. Energy-Delay-Deficiency product (EDDP) in Thermodynamic Computing

Let us outline the main ideas behind this work. We consider a driven system in contact with a thermal environ-

ment at temperature $k_B T = \beta^{-1}$. By suitably controlling the system’s potential $V(x, t)$, the dissipative dynamics leads to a state of the system that encodes the solution of a given computation. This constitutes a *thermodynamic algorithm* which consists of two basic steps (see also Fig. 1):

1. The system’s potential $V(x, t)$ is driven¹ from $V_0(x) := V(x, 0)$ to $V_1(x) := V(x, \tau_D)$ in a fixed amount of time τ_D , and as a consequence the system evolves from the distribution $\rho_0(x)$ into a target distribution $\rho_1(x)$ which encodes the solution of the problem. Often, $\rho_1(x)$ will correspond to a Gibbs state, namely

$$\rho_1(x) \propto e^{-\beta V_1(x)}. \quad (1)$$

2. The system is measured and samples are collected during a fixed amount of time τ_S . The outcome of the algorithm is given by

$$\langle f(x) \rangle = \frac{1}{\tau_S} \int_{\tau_D}^{\tau_D + \tau_S} dt' f(x(t')). \quad (2)$$

In the Markovian regime, we expect the error in the estimation in Step 2 to typically decay as $\sim 1/\tau_S$ and, in turn, the irrecoverable energy required to perform Step 1 decays as $\sim 1/\tau_D$ (see below). This clearly indicates a trade-off between the accuracy, energy, and total time $\tau := \tau_D + \tau_S$ of the computation. In order to account for all relevant resources, we will thus gauge the performance of thermodynamic algorithms via an extension of the well-known energy-delay-product (EDP) [52], namely a quantity of the form,

$$\text{EDDP} := W_{\text{diss}} \tau (1 - \mathcal{Q}) \quad (3)$$

¹ We consider any possible time-control protocol, including both continuous protocols but also sudden quenches (followed by equilibration processes where $V(x)$ remains constant).

Here, W_{diss} is the irrecoverable energy (dissipated work) and $0 \leq \mathcal{Q} \leq 1$ is a suitably defined quality factor. We will refer to the quantity from [eq. \(3\)](#) as the *energy-delay-deficiency product* (EDDP).

In what follows, we will quantify this tradeoff for thermodynamic hardware based upon a driven overdamped classical system [\[4, 40, 53\]](#), and argue that similar tradeoffs are valid as well for other physical platforms. Specifically, we will derive fundamental lower bounds to the EDDP and develop simple driving protocols with good-but-not-optimal performance. The key steps in our proofs draw from recent technical results in stochastic thermodynamics [\[47\]](#) which lower bound the energy required to thermodynamically drive between any two states of the system.

III. Thermodynamic computing in Langevin systems and bounds on EDDP

In the core of this work we consider, as base playground for the optimization of thermal computing protocols, physical systems whose dynamics is well described by the so-called (overdamped) Langevin equation [\[54\]](#). In terms of the particles' position vector x and energy potential $V(x, t)$, this reads as

$$\dot{x} = -\frac{1}{\gamma} \nabla V(x, t) + \sqrt{\frac{2}{\gamma\beta}} \eta(t), \quad (4)$$

where γ is a friction coefficient, and $\eta(t)$ is a white noise vector satisfying $\langle \eta_i(t) \eta_j(t') \rangle = \delta_{ij} \delta(t - t')$. This equation models systems in which particles' momentum relaxes rapidly, such as colloidal particles in a viscous medium, however notice that several systems have been shown to be well described by the same dynamical equation [\[55\]](#), such as particles in noisy optical traps [\[56\]](#), as well as overdamped RLC circuits [\[40, 55\]](#).

For a fixed potential $V(x, t) \equiv V(x)$ the probability distribution of the system tends to the thermal state represented by the Gibbs-Boltzmann distribution

$$\rho^{\text{th}}(x) = \frac{1}{Z} e^{-\beta V(x)}, \quad (5)$$

where Z simply corresponds to the normalization of the exponential distribution $Z \equiv \int dx e^{-\beta V(x)}$. The thermodynamics of this and more general stochastic systems has been well characterized [\[57, 58\]](#). Specifically, the internal energy U , work δW and heat δQ entering the system can be expressed as

$$E = \int dx \rho(x) V(x), \quad (6)$$

$$\delta W = \int dx \rho(x) \delta V(x), \quad (7)$$

$$\delta Q = \int dx \delta \rho(x) V(x), \quad (8)$$

where $\delta E = \delta W + \delta Q$ is the first law of thermodynamics.

Step 1 of a thermodynamic algorithm consists in a potential transformation $V_0(x) \rightarrow V_1(x)$ at constant surrounding temperature $k_B T = \beta^{-1}$. The overall work cost for such transformation is given by

$$W^{(0) \rightarrow (1)} = \Delta F + W_{\text{diss}}^{(0) \rightarrow (1)}, \quad (9)$$

where $\Delta F = F^{(1)} - F^{(0)}$ is the variation of the free energy $F = U - \beta^{-1} S$, with $S = -\int dx \rho(x) \ln \rho(x)$ being the entropy. It follows that $W_{\text{diss}}^{(0) \rightarrow (1)}$ is non-negative according to the second law of thermodynamics. **Step 2** of a thermodynamic algorithm consist in sampling the position of the particle x which does not modify the energetics of the system. Therefore, no work is performed in this step and control parameters are held fixed. Notice that the variation in free energy, ΔF , can always be recovered by complementing the protocol with a (sufficiently slow) reversible reset transformation taking $V_1(x) \rightarrow V_0(x)$. In principle, one could also consider more general sequential protocols in which $\{\rho_1^{\text{th}}, V_1\}$ produced in a previous run is treated as the new initialization for a following run, and so on; the total work required to perform m such thermodynamic algorithms correspond to a sum of contributions for each step, that is

$$\sum_{i=1}^m W^{(i-1) \rightarrow (i)} = \sum_{i=1}^m \Delta_i F + \sum_{i=1}^m W_{\text{diss}}^{(i-1) \rightarrow (i)} \quad (10)$$

$$= F^{(m)} - F^{(0)} + \sum_{i=1}^m W_{\text{diss}}^{(i-1)}, \quad (11)$$

where $\Delta_i F := F^{(i)} - F^{(i-1)}$. Once again, the global term $F^{(m)} - F^{(0)}$ (which can have any sign) is null in case $V_0 \equiv V_m$, or can be made null via a reversible transformation at the end. Finally, in case an infinitely slow reset is forbidden, e.g. due to time constraints, one can still perform the $V_1 \rightarrow V_0$ reset in finite time, by reversing the forward protocol. It can be shown (cf. [eq. \(23\)](#)) that in such case $W_{\text{diss}}^{(0) \rightarrow (1)} = W_{\text{diss}}^{(1) \rightarrow (0)}$, and thus the total energy expenditure of the full protocol would be $2W_{\text{diss}}^{(0) \rightarrow (1)}$.

For all these reasons, in the following we will consider the dissipation during **Step 1**, namely

$$W_{\text{diss}} := W_{\text{diss}}^{(0) \rightarrow (1)}, \quad (12)$$

to be the fundamental energy cost associated with a thermodynamic algorithm.

A. Wasserstein geometry and fundamental bounds on EDDP

We now introduce the main technical tool needed to derive our optimal EDP-like trade-offs. The energy cost W_{diss} is, in general, protocol-dependent and requires a full solution of the dynamical equations in order to be estimated. However, one can still obtain valuable insights with the help of geometry: a key result from Ref. [\[50, 51\]](#) shows that for systems governed by Langevin equation

from [eq. \(4\)](#), the dissipation W_{diss} can be bounded by the square of the Bures-Wasserstein distance \mathcal{W} between the initial and final distributions, $\rho_0 := \rho_0(x)$ and $\rho_1 := \rho_1(x)$, that is defined as

$$\mathcal{W}^2(\rho_0, \rho_1) := \inf_{\pi \in \Pi(\rho_0, \rho_1)} \int_{\mathbb{R}^n \times \mathbb{R}^n} |x - y|^2 d\pi(x, y), \quad (13)$$

where $\Pi(\rho_0, \rho_1)$ is the set of all probability density functions (so-called transport plans) having ρ_0 and ρ_1 as marginals [\[59\]](#). According to Ref. [\[50, 51\]](#), isothermal transformations of overdamped Langevin systems universally satisfy

$$W_{\text{diss}} \geq \frac{1}{\beta \gamma \tau_D} \mathcal{W}^2(\rho_0, \rho_1). \quad (14)$$

This inequality captures a key physical insight: faster protocols *necessarily* incur larger dissipation. In principle, the dissipation W_{diss} can even vanish in the limit $\tau_D \rightarrow \infty$, reflecting the reversibility of infinitely slow processes. Crucially, [eq. \(14\)](#) can be saturated by protocols in which the instantaneous distribution ρ_t follows the geodesic path in terms of Bures-Wasserstein distance between ρ_0 and ρ_1 [\[50, 51\]](#).

The above connection recasts the thermodynamic task of identifying a minimally dissipative protocol as a geometric problem. In particular, [eq. \(14\)](#) immediately provides the ultimate bound on the EDP restricted to **Step 1**—namely $W_{\text{diss}} \tau_D$ —solely in terms of the temperature, the friction coefficient, and the distance \mathcal{W} covered by the desired computation. Moreover, consider now the sampling **Step 2**. It is safe to assume (for example, if the sampling rate is sufficiently larger than γ^{-1}) that the result of the computation $\langle f(x) \rangle$ will have, for finite time τ_S , an estimation error

$$\varepsilon^2 := \left(\frac{1}{\tau_S} \int_{\tau_D}^{\tau_D + \tau_S} dt' f(x(t')) - \int dx f(x) \rho_1(x) \right)^2 \propto \frac{1}{\tau_S}. \quad (15)$$

For a given total time $\tau = \tau_D + \tau_S$ it then follows that

$$\frac{\tau_S}{\tau_D + \tau_S} = \frac{\varepsilon_{\text{min}}^2}{\varepsilon^2} =: \mathcal{Q}, \quad (16)$$

where $\varepsilon_{\text{min}}^2$ corresponds to the minimum error achievable in case the entire time τ of the protocol was spent for **Step 2**—sending $\tau_D \rightarrow 0$ is, in principle possible, at the expense of an asymptotically large W_{diss} . Therefore, $0 \leq \mathcal{Q} \leq 1$ can be seen to represent the *quality factor* of the computation.

Using [eq. \(16\)](#), it follows that the EDP of **Step 1** coincides with the EDDP of the entire algorithm, that is $W_{\text{diss}} \tau_D = W_{\text{diss}} \tau (1 - \mathcal{Q})$. Combining this observation with the bound in [eq. \(14\)](#), we can now state our main result as an EDP-like bound for thermodynamic computing,

$$\text{EDDP} \geq \frac{\mathcal{W}^2(\rho_0, \rho_1)}{\beta \gamma}. \quad (17)$$

That is, as the quality \mathcal{Q} of the computation increases, the dissipated energy or the total time must increase. In the remainder of the paper, we will estimate \mathcal{W} for relevant classes of protocols and look for practical thermodynamic computations that are close to saturating the fundamental bound [\(17\)](#).

B. Lower bound on \mathcal{W} and quadratic systems

The Wasserstein distance $\mathcal{W}(\rho_0, \rho_1)$ between two arbitrary distributions, as defined in [eq. \(13\)](#), is in general nontrivial to estimate, particularly for large dimensions, so it is useful to bound it using only the first two moments. For that let us define

$$\mu_i = \int dx x \rho_i(x), \quad (18)$$

$$\Sigma_i = \int dx (x - \mu_i)(x - \mu_i)^T \rho_i(x). \quad (19)$$

Then, following Ref. [\[60\]](#), one can lower-bound the Wasserstein distance as

$$\mathcal{W}(\rho_0, \rho_1)^2 \geq |\mu_0 - \mu_1|^2 + \mathcal{BW}(\Sigma_0, \Sigma_1)^2, \quad (20)$$

$$\mathcal{BW}(\Sigma_0, \Sigma_1)^2 := \text{Tr} \left[\Sigma_0 + \Sigma_1 - 2(\Sigma_1^{1/2} \Sigma_0 \Sigma_1^{1/2})^{1/2} \right].$$

where the notation $\mathcal{BW}(\Sigma_0, \Sigma_1)$ defines the *Bures-Wasserstein distance* [\[61\]](#) computed for two covariance matrices Σ_0 and Σ_1 .

The bound [eq. \(20\)](#) is saturated in the case of Gaussian distributions moving along their corresponding Wasserstein geodesics. In the context of thermal equilibrium, Gaussian distributions are exactly those arising from quadratic potentials of the form

$$V(x) = \frac{1}{2} x^T K x + b^T x \quad (21)$$

which leads to the equilibrium distribution

$$p^{\text{th}}(x) = \frac{e^{-\frac{1}{2}(x - \mu)^T \Sigma^{-1}(x - \mu)}}{\sqrt{(2\pi)^N \det \Sigma}} \quad (22)$$

where $\Sigma = (\beta K)^{-1}$, and $\mu = -K^{-1}b$. Here K is a positive semi-definite matrix encoding pairwise interactions, and b is a vector describing linear energy terms. The thermodynamics of quadratic overdamped systems has been characterized in Ref. [\[46\]](#).

The corresponding entropy production can be then expressed from the integral over time of the euclidean metric for μ and the \mathcal{BW} metric for Σ , i.e.

$$\begin{aligned} \beta W_{\text{diss}} &= \int_0^\tau dt |\dot{\mu}(t)|^2 \\ &+ \frac{1}{2} \int_0^\tau dt \text{Tr} \left[\int_0^\infty d\nu e^{-\nu \Sigma(t)} \dot{\Sigma}(t) e^{-\nu \Sigma(t)} \dot{\Sigma}(t) \right]. \end{aligned} \quad (23)$$

In our applications, we will in general assume μ constant as it only provides an irrelevant shift of the distribution. Moreover one can often assume $\Sigma_0 \propto \mathbb{1}$,

which simplifies the analysis. In particular, when Σ_0 and Σ_1 commute, i.e., $[\Sigma_0, \Sigma_1] = 0$, the squared \mathcal{BW} distance decomposes into a sum over the eigenvalues $\sigma_{i,\alpha}$ of Σ_i , yielding the closed-form formula $\mathcal{BW}(\Sigma_0, \Sigma_1)^2 = \sum_\alpha (\sqrt{\sigma_{0,\alpha}} - \sqrt{\sigma_{1,\alpha}})^2$.

C. General optimization principles: symmetries and slow-driving

The expressions for the dissipated W_{diss} (23) and its achievable minimum \mathcal{BW} (20) will thus be central in the design of optimal and close-to-optimal protocols for (Gaussian) thermodynamic computing. Before dwelling into explicit protocols, it is worth discussing a few considerations.

First, as β^{-1} naturally sets the energy scale of the problem, it is easy to notice that the transformation $\beta^{-1} \rightarrow \lambda\beta^{-1}$ leads to $\Sigma(t) \rightarrow \lambda\Sigma(t)$ which, upon substitution into eq. (23), yields immediately $W_{\text{diss}} \rightarrow \lambda W_{\text{diss}}$. Thus, W_{diss} is *linear* in the temperature as expected.

Secondly, we can note that a scale invariance appears of the dissipation naturally emerges from eq. (23): for a given finite-time protocol $K(t)$ the dissipation remains constant for the transformation $K(t) \rightarrow K'(t) = \lambda K(\lambda t)$ (with $\tau_D \rightarrow \tau_D/\lambda$ and $\lambda > 0$), i.e. scaling it in magnitude by a factor λ and accelerating it by the same factor leaves the dissipation unchanged. In fact, one can see that given a solution $\Sigma(t)$ of the dynamics associated to the driving $K(t)$, the rescaled $\Sigma'(t) = \lambda^{-1} \Sigma(\lambda t)$ corresponds to a solution for $K'(t)$. Substituting this into eq. (23), the same transformation provides $W_{\text{diss}} \rightarrow W_{\text{diss}}$, which is therefore invariant under this time-strength rescaling (more details in App. B). This symmetry implies that amplifying the protocol's strength by λ while compressing its duration to τ/λ yields an equivalent thermodynamic outcome. This scaling symmetry defines an equivalence class in the family of protocols with the same EDDP. A direct consequence is that in principle one should use the highest value of λ allowed by the physical hardware at hand. Indeed, any computation encoded in $\rho_1(x)$ obtained from $\rho_0(x)$ is equivalently encoded in $\rho'_1(x) \propto \rho_1(\sqrt{\lambda}x)$ obtained from $\rho'_0(x) \propto \rho_0(\sqrt{\lambda}x)$ in a protocol pertaining to the same equivalence class. However any physical device will entail a maximum value of λ , due to both a finite achievable strength of the energy potential K , and a finite resolution when sampling from a distribution with spread Σ .

Finally, let us mention that we will often consider, in our analysis, the regime in which τ_D and τ_S are much larger than the thermalization rate γ^{-1} . In fact, a large τ_S is needed to yield a small computation error ε^2 , whereas a large τ_D enables the possibility of small dissipation according to eq. (14). In terms of dynamical driving this is often referred to as *slow-driving* regime [62–64], which assumes the rate of change of $V(x, t)$ in time is sufficiently slow to have the state $\rho(x, t)$ always close to the thermal $\rho^{\text{th}}(x)$ corresponding to $V(x, t)$. More specif-

ically one can expand

$$\Sigma(t) = \beta^{-1} K^{-1}(t) + \mathcal{O}\left(\frac{1}{\tau_D}\right) \quad (24)$$

and substitute it in eq. (23) to express W_{diss} up to $\mathcal{O}(\tau_D^{-2})$ corrections [46]. That is, in the slow-driving regime, we do not need to solve the dynamical equations for $\rho(x, t)$ and $\Sigma(t)$, rather we can express the thermodynamic performance directly in terms of the driving $K(t)$.

IV. EDDP of Protocols with limited control and available information

Up to this point, our analysis has focused on the controlled time evolution of the system's distribution $\rho(x, t)$. In practice, however, one cannot directly manipulate the system's state, but only its energy potential $V(x, t)$. In this section we will focus on characterizing and optimizing with different approaches and classes of protocols the EDP incurred during **Step 1** of the algorithm—and thus the EDDP of the algorithm as a whole—for Gaussian thermodynamic computing.

A. Quenches

Let us start by considering protocols that require the least amount of control and knowledge: quenches. These consist in an immediate and instantaneous transformation of the potential $V(x, 0) = V_0(x)$ to $V(x, 0^+) = V_1(x)$ with a fixed waiting time to let the system be sufficiently close to its equilibrium state once we start **Step 2**. The dissipated energy of these quenches is fixed by the boundary conditions of the protocol and does not depend on the waiting time for equilibration since we are assuming that the final state is close to equilibrium (cf. App. C)

$$W_{\text{diss}}^Q = \frac{1}{2} k_B T \left(\text{Tr}[K_1 K_0^{-1} - \mathbb{1}] + \ln \left[\frac{\det K_0}{\det K_1} \right] \right), \quad (25)$$

which leads an energy-delay-deficiency product that scales linearly with τ_D : $\text{EDDP}^Q = W_{\text{diss}}^Q \tau_D$.

B. Geodesics

However, the optimal achievable EDDP given by the Bures-Wasserstein distance does not scale with τ_D : $\min_{(K(t), \Sigma(t))} \text{EDDP} = \mathcal{BW}(\Sigma_0, \Sigma_1) / (\beta\gamma)$. From this minimal EDDP we can see how the constant $\beta\gamma$ sets the scale of the problem, which is a consequence of the symmetries discussed in the previous section. Since a rescaling of these constants does not affect the minimization problem, we will be setting $\beta = 1$ and $\gamma = 1$ for the rest of this section, to lighten the notation. The minimal EDDP is realized by the geodesic² state trajectory

$$\Sigma_{\text{geo}}(t) = \left(\frac{t}{\tau_D} \sqrt{\Sigma_1} + \frac{\tau_D - t}{\tau_D} \sqrt{\Sigma_0} \right)^2. \quad (26)$$

² It is called a geodesic since the length of this trajectory minimizes the Bures-Wasserstein distance.

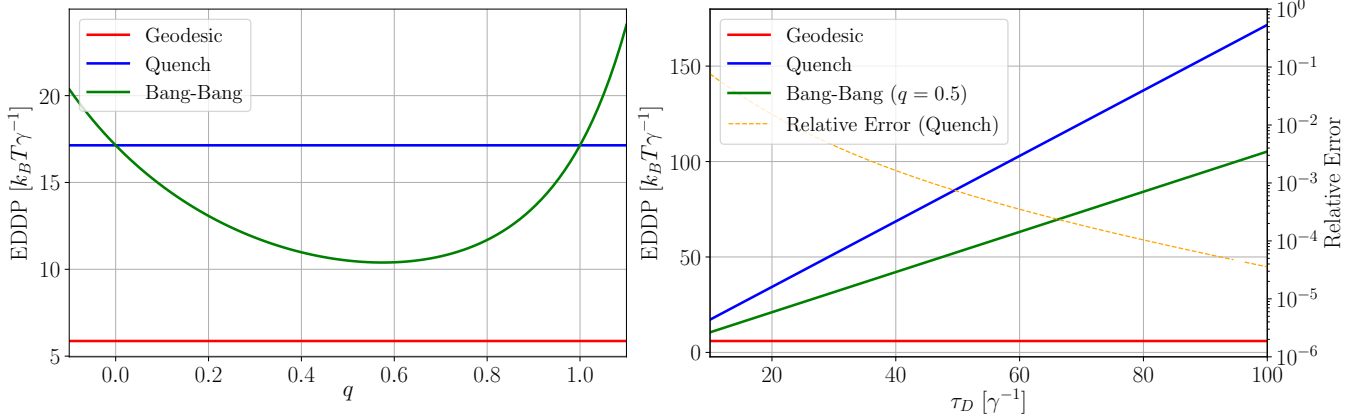


FIG. 2. Average EDDP for 500 samples of K_1 taken from a Wishart distribution of 10×10 matrices with expected value $K_0 = \mathbb{1}$ and 20 degrees of freedom. (Left) Comparison of the EDDP for geodesic, quench, and Bang-Bang protocols as a function of the interpolation parameter q for a driving time $\tau_D = 10\gamma^{-1}$. Qualitatively, the shape of the Bang-Bang EDDP curve remains the same as one increases the driving time. (Right) Comparison of the EDDP for geodesic, quench, and Bang-Bang with $q = 0.5$ protocols as a function of the driving time τ_D . And relative error of the quench protocol ($\sqrt{\text{Tr}[(\Sigma(\tau_D) - K_1^{-1})^2] / \text{Tr}[K_1^{-2}]}$) as a function of the driving time. The relative error of the Bang-Bang protocol is slightly larger (and dependent on q) but is of the same order.

This trajectory can be obtained with the following control (cf. App. C)

$$K_{\text{geo}}(t) = \left[\mathbb{1} - \frac{\chi_{(0, \tau_D)}(t)}{\tau_D} \Delta_{\text{geo}}(t) \right] \Sigma_{\text{geo}}(t)^{-1}, \quad (27)$$

$$\Delta_{\text{geo}}(t) := \frac{t}{\tau_D} \Sigma_1 + \frac{\tau_D - 2t}{\tau_D} \sqrt{\Sigma_1} - \frac{\tau_D - t}{\tau_D} \mathbb{1} \quad (28)$$

with $\chi_{(0, \tau_D)}(t)$ the indicator function of the open interval $(0, \tau_D)$. Furthermore, this protocol has another advantage compared to the naive quench: it reaches exactly the desired state with covariance matrix Σ_1 at τ_D . The geodesic protocol achieves this property by “overshooting” the final control K_1 in such a way that at $t = \tau_D$ the state can reach Σ_1 (instead of converging asymptotically to it) and then making a quench “back to” K_1 .

However, both the continuous part and the quenches of this geodesic control trajectory require knowledge of Σ_1 . In general, the objective of the algorithm is precisely to extract information from the distribution ρ_1 . Therefore, we will have to assume that we do not have prior knowledge of this distribution—thus of Σ_1 —and cannot implement the geodesic protocol in Step 1.

C. Bang-bang protocols

In what follows we will study how much we can improve on the quenches protocol and get close to the minimal EDDP with protocols that only require interpolations of the matrices K_0 and K_1 . In the interest of outlining what we have access to and what we don’t, we will evaluate the EDDP of these protocols in the case study of a specific algorithm: matrix inversion. In this case we are given as input the matrix K_1 and desire to compute its inverse. Since the covariance matrix of the thermal state is given by $\Sigma_{th} = K^{-1}$, to compute the inverse in Step 1 we drive the control from K_0 to K_1 , and then we reconstruct the covariance matrix by sampling the position of the colloidal particles during Step 2. Using the

scale symmetries of the cost (outlined in Sec. III C and detailed in App. B), we notice that we can take, up to a scalar renormalization of the entire problem, $K_0 = \mathbb{1}$. Moreover, partial knowledge on the set of matrices from which K_1 is sampled, can also be used to optimize the initialization scale $K_0 = \mathbb{1} \rightarrow K_0 = \lambda \mathbb{1}$, see App. D.

One of the simplest improvements one can obtain from the quenches is to split these in two steps, as it has been shown that the energy-optimal protocols for rapidly driven systems are “bang-bang” protocols [65]. The procedure consists in a first quench at $t = 0$ from the initial control K_0 to an intermediary control K_* , followed by letting the system thermalize for $\tau_D/2$, then a second quench to the final control K_1 and letting the system relax for the remaining time $\tau_D/2$. We obtain that the dissipated work is (cf. App. C)

$$W_{\text{diss}}^{\text{Bang-Bang}} = W_{\text{diss}}^Q - \frac{1}{2} \text{Tr}[(K_1 - K_*)(K_0^{-1} - \Sigma_*)], \quad (29)$$

where $\Sigma_* = e^{-K_* \tau_D/2} \Sigma_0 e^{-K_* \tau_D/2} + (\mathbb{1} - e^{-K_* \tau_D}) K_*^{-1}$ is the covariance of the state at $t = \tau_D/2$. Since we restrict ourselves to only have access to interpolations of K_0 and K_1 we can naturally write the intermediary control as $K_* = q K_1 + (1 - q) K_0$, where q is the interpolation parameter. To evaluate the performance of this protocol we compute its corresponding EDDP for instances of K_1 sampled from a Wishart distribution with mean $K_0 = \mathbb{1}$. In Fig. 2 we showcase the mean EDDP for the Bang-Bang protocol, the quench protocol, and the geodesic protocol as a function of the interpolation parameter q and as a function of the driving time τ_D . We only consider driving times larger than $10\gamma^{-1}$ since we need the $\Sigma(\tau_D)$ to be relatively close to the desired thermal state K^{-1} for the quench and Bang-Bang protocols (for the geodesic protocol the error is null). We quantify the relative error with the Hilbert-Schmidt norm

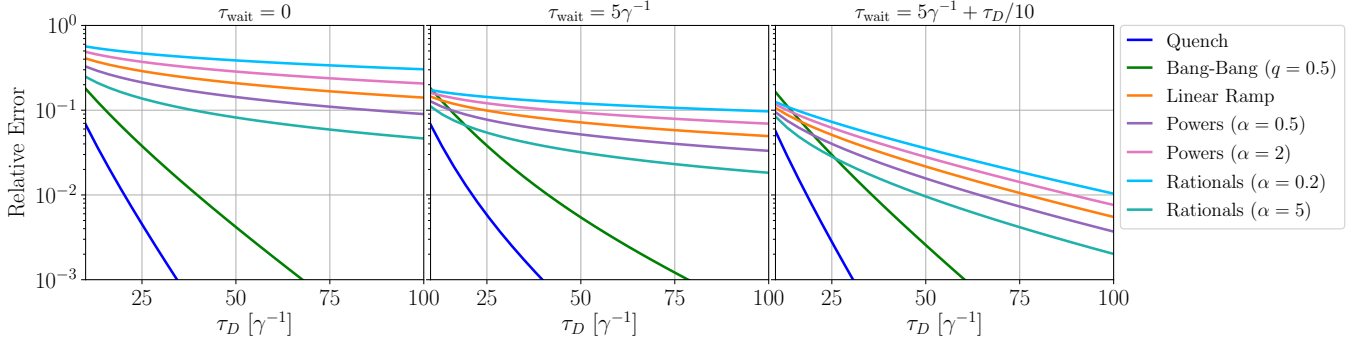


FIG. 3. Average Relative error ($\sqrt{\text{Tr}[(\Sigma(\tau_D) - K_1^{-1})^2] / \text{Tr}[K_1^{-2}]}$) for 100 samples of K_1 taken from a Wishart distribution of 10×10 matrices with expected value $K_0 = \mathbb{1}$ and 20 degrees of freedom. The relative error is shown for the different protocols as a function of τ_D ($\tau_D \in [10\gamma^{-1}, 100\gamma^{-1}]$) for multiple values of τ_{wait} : (Left) no relaxation time, (Middle) fixed waiting time, (Right) adaptive waiting time.

$\sqrt{\text{Tr}[(\Sigma(\tau_D) - K_1^{-1})^2] / \text{Tr}[K_1^{-2}]}$. Overall, we can observe that the Bang-Bang protocol yields a significant improvement when the interpolation parameter is around $q \approx 0.5$. However, the scaling of the EDDP with respect to τ_D remains linear.

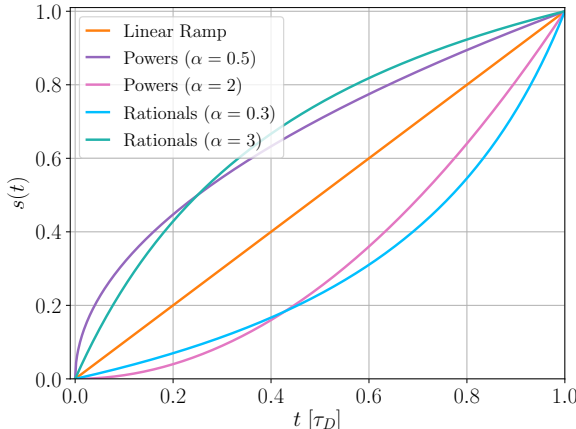


FIG. 4. Examples of continuous driving functions for the Powers and Rationals families.

D. Continuous protocols

We can make a more sophisticated improvement by considering protocols that drive the control continuously from K_0 to K_1 . Since we restrict ourselves to interpolations of the boundary conditions, we can write such protocols as $K(t) = s(t)K_1 + (1 - s(t))K_0$, where $s(t)$ is a bijective non-decreasing³ map from $[0, \tau_D]$ to $[0, 1]$. Here, we will consider two families of functions for $s(t)$:

$$s_{\text{Powers}}(t) = \frac{t^\alpha}{\tau_D^\alpha}, \quad (30)$$

$$s_{\text{Rationals}}(t) = \frac{\alpha t}{\tau_D + (\alpha - 1)t}, \quad (31)$$

³ Given the geometric nature of the problem, it is immediate that non-bijective maps do not need to be considered in this problem since for any non-bijective map one can trivially construct a bijective map that will have a smaller dissipation.

for $\alpha > 0$ a free parameter. At $\alpha = 1$ these functions coincide with a linear ramp: $K(t) = \frac{t}{\tau_D}K_1 + \frac{\tau_D - t}{\tau_D}K_0$. We present a visualization of a few examples of protocols in these families in Fig. 4. It is worth noting that none of these will universally approximate well the geodesics. Indeed, if we consider the concavity of the optimal control $K_{\text{geo}}(t)$ in eq. (27) for scalars (i.e. by taking the trivial case of 1×1 matrices) we can see that it is always convex in the bulk. While for these families of interpolated protocols, the convexity switches to concavity (and vice-versa) when $K_0 - K_1$ changes sign.

As it was alluded to in the discussion above, unless the driving time τ_D is large compared to the thermalization timescale γ^{-1} the state of the system at the end of Step 1 will not be close enough to the thermal distribution to start the sampling in Step 2. Therefore, before analyzing the EDDP of the continuous protocols, we start by analyzing the relative error they yield at the end of Step 1. By eq. (24) the relative error of $\Sigma(\tau_D)$ scales as $(\gamma\tau_D)^{-1}$ for the continuously driven protocols. However, it is worth noting that once the control is fixed at K_1 the state converges exponentially fast to the thermal distribution. Therefore for the quench and bang-bang protocols the error scales as $e^{-\gamma\tau_D}$. By the same reasoning, any error that is present at the start of Step 2 will also be suppressed exponentially fast during the sampling since the state keeps thermalizing during the sampling.

In order to minimize the error, we can also exploit this exponential relaxation for continuously driven protocols by dedicating some of the driving time solely to thermalization. More precisely, we can subdivide the Step 1 of continuously driven protocols in two parts: a. driving the system continuously from K_0 (at $t = 0$) to K_1 (at $t = \tau_D - \tau_{\text{wait}}$), b. let the system thermalize for a duration τ_{wait} (from $t = \tau_D - \tau_{\text{wait}}$ to $t = \tau_D$). In Fig. 3 we show the relative error of $\Sigma(\tau_D)$ as a function of τ_D for different amounts of waiting time. In the left panel, we can see that since the error of the continuously driven protocols decays slowly (compared to the quench and bang-bang protocols), it takes significantly long protocols to obtain a reasonable relative error when there is no waiting time. By adding a constant waiting time

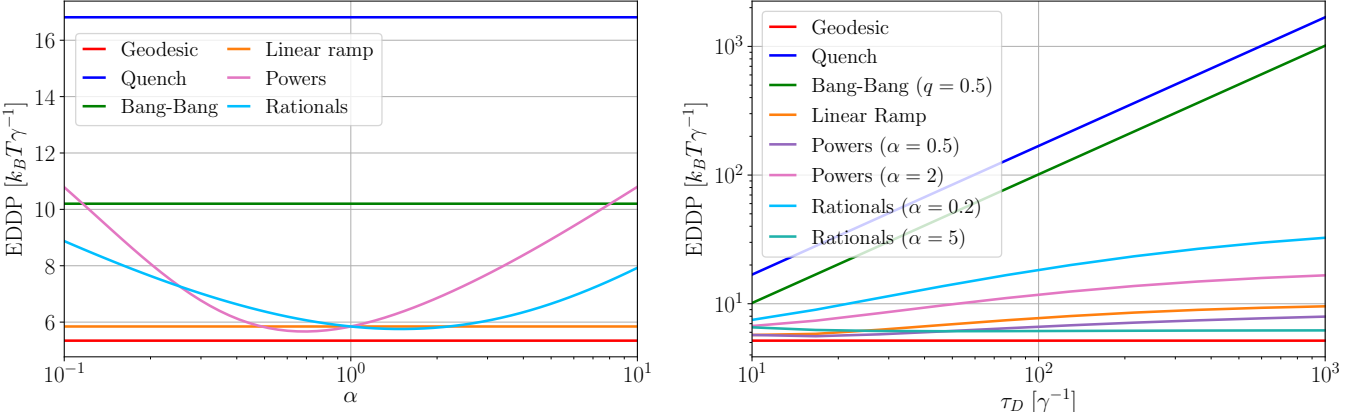


FIG. 5. Average EDDP for 100 samples of K_1 taken from a Wishart distribution of 10×10 matrices with expected value $K_0 = 1$ and 20 degrees of freedom. (Left) EDDP of the Powers, and Rationals protocol families as a function of the free parameter α with $\tau_D = 10\gamma^{-1}$ and $\tau_{\text{wait}} = 5\gamma^{-1}$. These are compared to the EDDP of the geodesic, quench, Bang-Bang ($q = 0.5$), and linear ramp protocols. (Right) Comparison of the EDDP for a collection of protocols as a function of τ_D .

(middle panel) we improve the situation by a constant factor, however the scaling remains the same. The scaling can be improved by taking a τ_{wait} that scales with τ_D (right panel), which will allow for an exponential decay of the error as in the quench and bang-bang protocols. In what follows, we will restrict ourselves to cases with a constant waiting time as it is sufficient for our analysis to have a reasonably small relative error at the end of **Step 1**.

In Fig. 5 we study how the EDDP of these continuous protocols changes depending on the free parameter α and compare it to the performance of the geodesic, quench, and Bang-Bang protocols. We can see that for relatively fast protocols ($\tau_D = 10$ in the left panel) the continuous protocols perform much better than the quenches and Bang-Bang as they are quite close to the geodesic. Furthermore the linear ramp, which is also the most naive guess for a continuous protocol, is close to optimal for both families of protocols. In terms of scaling with respect to τ_D the continuous protocols perform significantly better than the quench and Bang-Bang protocols. From the right panel we can clearly see that the EDDP of the continuous protocols scales sub-linearly with τ_D . However, we can further prove that it converges to a constant in the slow driving limit: by inserting eq. (24) into eq. (23) and using the fact that $[K(t), K(t')] = 0$ along these protocols (since we chose $K_0 = 1$) we find

$$\text{EDDP} = \frac{\tau_D}{4} \int_0^{\tau_D} dt \text{Tr} \left[\frac{\dot{K}(t)^2}{K(t)^3} \right] + \mathcal{O}\left(\frac{1}{\tau_D}\right). \quad (32)$$

By construction, the interpolation is such that $\dot{s}(t) \propto \tau_D^{-1}$, therefore we can show that the leading order of eq. (32) is independent of τ_D . Furthermore, since the sampling time τ_S in **Step 2** needs to be much larger γ^{-1} , we are free to assume the same for τ_D and enter the slow-driving regime (while still being able to keep it small compared to τ_S and keeping a large quality factor Q). In this scenario, we can ignore the waiting time since in the slow driving regime the state of the system remains close

to the thermal distribution throughout the protocol.

E. Slow driving protocols

Since for the quench and Bang-Bang protocols EDDP scales with τ_D , it diverges in the slow-driving regime. Therefore, we cannot compare it to the EDDP of the continuous protocols. In Fig. 6 we study the EDDP in the slow-driving regime for the different continuous protocols as a function of the free parameter α and the dimension of the matrices. Generally, we can notice that most continuous protocols we consider perform relatively close to the optimal EDDP given by the geodesic. For example, the Rationals protocol with $\alpha \approx 4$ is significantly close to the theoretical optimum. It is also worth noting that we can trade-off EDDP for simplicity by implementing the Linear Ramp protocol, which performs with approximately double the EDDP of the geodesic. We also study how the EDDP depends on the matrix dimension d , observing a linear scaling that emerges as the dimension of the matrix increases, and that it is highly dependent on the specific protocol. Indeed, this can be proven from eq. (32): since the protocol satisfies $[K(t), K(t')] = 0$ we can rewrite it as a sum over the eigenvalues $k_i(t)$ of $K(t)$

$$\text{EDDP} = \frac{\tau_D}{4} \sum_{i=1}^d \int_0^{\tau_D} dt \frac{\dot{k}_i(t)^2}{k_i(t)^3} + \mathcal{O}\left(\frac{1}{\tau_D}\right). \quad (33)$$

Since the eigenvalues are identically distributed we can show that the EDDP scales linearly with the dimension as d becomes large (cf. App. C). We can therefore analyze the scaling of the slow-driving EDDP as a function of the free parameter α , which we show in Fig. 7. What we can observe is very similar to what we have found already for $d = 10$, however, the protocol that gets closest to the theoretical optimum becomes the rational protocol with $\alpha \approx 3.2$.

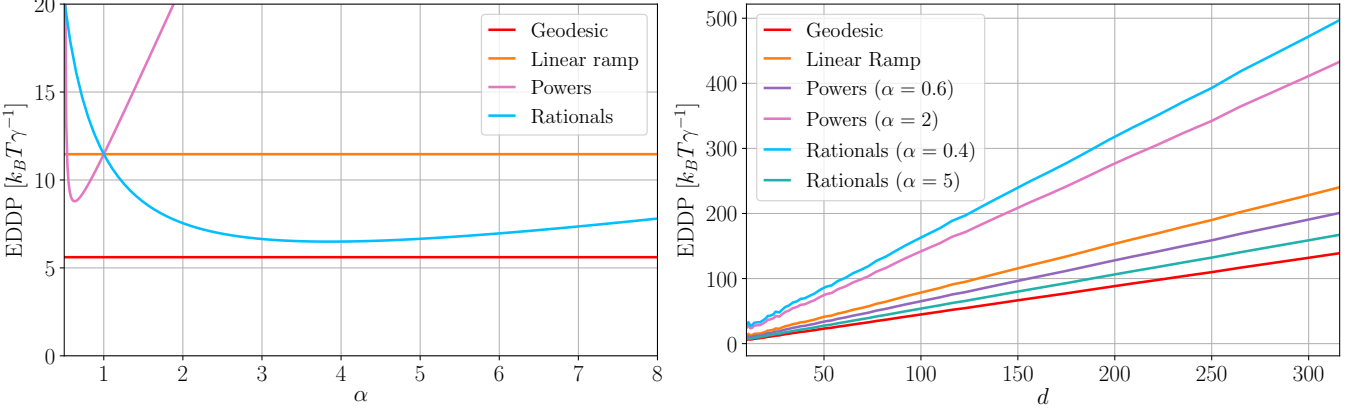


FIG. 6. Average EDDP in the slow-driving regime for 200 samples of K_1 taken from a Wishart distribution of $d \times d$ matrices with expected value $K_0 = 1$ and $2d$ degrees of freedom. (Left) EDDP of the Powers, and Rationals protocol families as a function of the free parameter α with $d = 10$. These are compared to the EDDP of the geodesic and linear ramp protocols. (Right) Comparison of the EDDP for a collection of protocols as a function of the matrix dimension d .

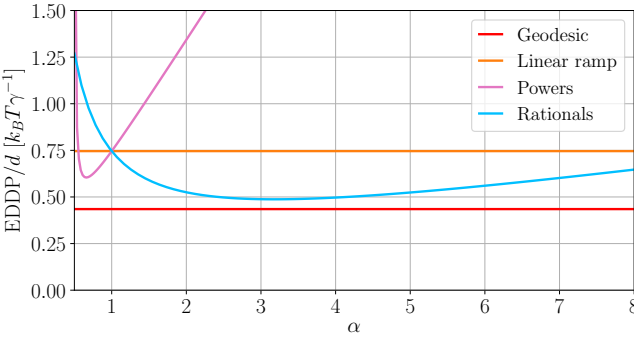


FIG. 7. Average scaling of the slow-driving EDDP as a function of the matrix dimension d (i.e. EDDP/d) for 150 samples of K_1 taken from a Wishart distribution of $d \times d$ matrices with expected value $K_0 = 1$ and $2d$ degrees of freedom. We compare the EDDP scaling for the Powers, and Rationals protocol families as a function of the free parameter α . These are compared to the EDDP scaling of the geodesic and linear ramp protocols.

V. EDDP bounds for arbitrary time-dependent potentials and thermodynamic neural networks

We now summarize how our geometric approach for quantifying the EDDP trade-off extends beyond the overdamped Brownian particle in a quadratic potential. The same geometric approach, namely measuring entropy production via a transport distance, applies to arbitrary potentials, to underdamped (phase-space) Langevin dynamics, and even to discrete Markov jump processes, albeit with important caveats on computability and tightness. Below we discuss these extensions in greater detail.

In this regime, we retain the overdamped Langevin model from eq. (4), but now allow for an arbitrary potential $V(x, t)$. The resulting bound on entropy production

keeps the same structure, namely,

$$W_{\text{diss}} \geq \frac{1}{\beta \gamma \tau_D} \mathcal{W}^2(\rho_0, \rho_1), \quad (34)$$

In practice, the transport distance \mathcal{W} can be difficult to compute for general (non-Gaussian) $\rho_{0,1}$. Importantly, the bound on the Bures-Wasserstein distance from eq. (20) is valid for arbitrary potentials and uses only the first two moments of the distribution, namely

$$\mathcal{W}^2(\rho_0, \rho_1) \geq \|\mu_0 - \mu_1\|^2 + \text{Tr} \Sigma_0 + \text{Tr} \Sigma_1 - 2 \text{Tr} [(\Sigma_0^{1/2} \Sigma_1 \Sigma_0^{1/2})^{1/2}], \quad (35)$$

with $\mu_{0,1}$ and $\Sigma_{0,1}$ being the means and covariances of $\rho_{0,1}$. This allows us to bound the EDDP product even when the endpoints of the protocol are not simply Gaussian states, which occurs when the driving protocol is non-quadratic.

Indeed, not all thermodynamic algorithms require access to a Gibbs state. Recent work in this direction, see in particular Refs. [36, 49, 66], show an interesting way to use Langevin dynamics for computation using arbitrary potentials, with sampling occurring at a chosen observational time, i.e. without requiring full equilibration. We discuss this approach briefly below in the context of our results.

Thermodynamic neural networks provide an example of a useful Langevin-based computation that does not require full equilibration and does not rely on quadratic potentials [49]. A single thermodynamic neuron is a scalar degree of freedom confined by a higher-order potential given by

$$U_J(x, I) = -Ix + J_2 x^2 + J_3 x^3 + J_4 x^4, \quad (36)$$

where $J = (J_2, J_3, J_4)$ specifies the couplings and I denotes an input (bias) signal. Networks are formed by

coupling such neurons via bilinear terms so that the total potential of the device reads

$$V(x, I) = \sum_i U_J(x_i, b_i) + \sum_{\langle i, j \rangle} J_{ij} x_i x_j + \sum_{i,j} W_{ij} I_i x_j. \quad (37)$$

The time evolution of such a device is governed by the overdamped Langevin dynamics from [eq. \(4\)](#). In this paradigm one trains the network using e.g. gradient-based method on a digital device, so that the thermodynamic device produces a desired function of the input at a prescribed measurement time τ_M . This output is obtained similar to the protocols discussed in this work, that is, sampling the network at the measurement time τ_M and then averaging.

In the context of our results, this class of finite-time computations also obeys a similar type of EDDP as in [eq. \(17\)](#) that trades sampling time, dissipation and quality of computation. The only difference is that now the lower bound on dissipation from [eq. \(14\)](#) must be expressed in terms of the distance between the actual distributions that characterize the device at the initial and final point of the driving protocol. It would be interesting to see if the driving protocols discussed in [Sec. IV](#) (e.g. the [Rationals protocol](#)) are also close to the optimal protocol specified by the geodesic.

Finally, we note that the considered bounds can also be extended to underdamped dynamics and discrete systems. In the former case, the over-damped bounds from [eq. \(34\)](#) can be applied to the position marginals of the phase-space densities. This yields valid lower bounds on dissipation, but momentum degrees of freedom typically prevent the corresponding bound from being tight. Similar geometric bounds for discrete systems have been discussed in [Ref. \[67\]](#). Importantly, they admit useful lower bounds by operational metrics (e.g. total variation or relative entropy bounds), which can yield model-independent estimates of minimal dissipation for discrete thermodynamic algorithms.

VI. Conclusion and Outlook

In this work, we characterized the energy–delay product (EDP) of thermodynamic algorithms based on Langevin dynamics, in which dissipative evolution naturally drives the system toward the solution of the computation. We first derived general bounds on the energy–delay–deficiency product (EDDP)—a generalization of EDP that incorporates the stochastic nature of thermodynamic computing—by exploiting geometric bounds on dissipation [\[50, 51\]](#). Although these bounds

can, in principle, be saturated by physical evolutions, the corresponding optimal driving protocols require knowledge of the final equilibrium state, i.e., the solution itself. This motivated the development of quasi-optimal protocols using only partial information and limited control, which we demonstrated in the context of matrix inversion. The derived protocols do not require prior information and approach the fundamental thermodynamic limits.

While our analysis focused on linear inversion problems for overdamped quadratic systems, the EDDP bounds extend to general potentials and to underdamped dynamics—although they are tight only for quadratic Hamiltonians and Gaussian states [\[46\]](#). In particular, they apply directly to the recently proposed framework of thermodynamic networks in [Ref. \[49\]](#).

Looking ahead, it is natural to explore similar trade-offs in other models of thermodynamic computation beyond Langevin systems, e.g., [Refs. \[68, 69\]](#), and in physics-based computing more broadly. Related energetic constraints have already been observed in minimal thermodynamic logic gates [\[17–19\]](#) and in energy-based machine learning models [\[70\]](#). The generalized EDDP provides a natural metric to capture such trade-offs, and we expect that unifying principles—analogous in spirit to thermodynamic uncertainty relations—may ultimately yield general bounds on EDDP across a wide class of physical computing architectures. Such results could offer concrete guidelines for designing computing hardware and algorithms that operate closer to the fundamental energetic limits.

Acknowledgments

We warmly thank Nicolas Brunner, Sadra Boreiri, Jake Xuereb, Sam Duffield, and Denis Melanson for fruitful and insightful discussions.

A.R. acknowledges funding from the Swiss National Science Foundation (Postdoc.Mobility grant ‘CATCH’ P500PT225461) and from the European Research Council (Consolidator grant ‘Cocoquest’ 101043705). P.A. acknowledges fundings from the Austrian Science Fund (FWF) projects I-6004 and ESP2889224. P.L.-B. acknowledges funding from the Polish National Science Centre through project Sonata 2023/51/D/ST2/02309. M.P.-L. acknowledges support from the Grant ATR2024-154621 funded by the Spanish MICIU/AEI/10.13039/501100011033. M.A. and P.J.C. acknowledge funding from the Advanced Research and Invention Agency’s (ARIA) Scaling Compute programme.

[1] J. Burr and A. Peterson, *Idaho Univ., The 1991 3rd NASA Symposium on VLSI Design*, Tech. Rep. (NASA, 1991).

[2] D. Marković, A. Mizrahi, D. Querlioz, and J. Grollier, Physics for neuromorphic computing, *Nature Reviews Physics* **2**, 499 (2020).

[3] T. Conte, E. DeBenedictis, N. Ganesh, T. Hylton, J. P. Strachan, R. S. Williams, A. Alemi, L. Altenberg, G. Crooks, J. Crutchfield, L. del Rio, J. Deutsch, M. DeWeese, K. Douglas, M. Esposito, M. Frank, R. Fry, P. Harsha, M. Hill, C. Kello, J. Krichmar, S. Kumar, S.-C. Liu, S. Lloyd, M. Marsili, I. Nemenman, A. Nugent, N. Packard, D. Randall, P. Sadowski, N. Santhanam, R. Shaw, A. Stieg, E. Stopnitzky, C. Teuscher, C. Watkins, D. Wolpert, J. Yang, and Y. Yufik, *Thermodynamic computing* (2019).

[4] P. J. Coles, C. Szczepanski, D. Melanson, K. Donatella, A. J. Martinez, and F. Sbahi, Thermodynamic ai and the fluctuation frontier, in *2023 IEEE International Conference on Rebooting Computing (ICRC)*, IEEE (IEEE, 2023) pp. 1–10.

[5] R. Landauer, Irreversibility and heat generation in the computing process, *IBM Journal of Research and Development* **5**, 183 (1961).

[6] E. Friedman, Clock distribution networks in synchronous digital integrated circuits, *Proceedings of the IEEE* **89**, 665 (2001).

[7] A. Chandrakasan, S. Sheng, and R. Brodersen, Low-power cmos digital design, *IEEE Journal of Solid-State Circuits* **27**, 473 (1992).

[8] K. Roy, S. Mukhopadhyay, and H. Mahmoodi-Meimand, Leakage current mechanisms and leakage reduction techniques in deep-submicrometer cmos circuits, *Proceedings of the IEEE* **91**, 305 (2003).

[9] M. Horowitz, 1.1 computing’s energy problem (and what we can do about it), in *2014 IEEE International Solid-State Circuits Conference Digest of Technical Papers (ISSCC)*, IEEE (IEEE, 2014) pp. 10–14.

[10] D. H. Wolpert, J. Korbel, C. W. Lynn, F. Tasnim, J. A. Grochow, G. Kardeş, J. B. Aimone, V. Balasubramanian, E. De Giuli, D. Doty, N. Freitas, M. Marsili, T. E. Ouldridge, A. W. Richa, P. Riechers, E. Roldán, B. Rubenstein, Z. Toroczkai, and J. Paradiso, Is stochastic thermodynamics the key to understanding the energy costs of computation?, *Proceedings of the National Academy of Sciences* **121**, 2321112121 (2024).

[11] P. Chattopadhyay, A. Misra, T. Pandit, and G. Paul, Landauer principle and thermodynamics of computation, *Reports on Progress in Physics* **88**, 086001 (2025).

[12] P. Chattopadhyay and G. Paul, Understanding the thermodynamics of computation: a pedagogical overview, *Quantum Information Processing* **24**, 305 (2025).

[13] K. Proesmans, J. Ehrich, and J. Bechhoefer, Finite-time landauer principle, *Physical Review Letters* **125**, 100602 (2020).

[14] T. Van Vu and K. Saito, Finite-time quantum landauer principle and quantum coherence, *Physical Review Letters* **128**, 010602 (2022).

[15] A. Rolandi and M. Perarnau-Llobet, Finite-time landauer principle beyond weak coupling, *Quantum* **7**, 1161 (2023).

[16] P. Taranto, F. Bakhshinezhad, A. Bluhm, R. Silva, N. Friis, M. P. Lock, G. Vitagliano, F. C. Binder, T. Debarba, E. Schwarzhans, F. Clivaz, and M. Huber, Landauer versus nernst: What is the true cost of cooling a quantum system?, *PRX Quantum* **4**, 010332 (2023).

[17] D. H. Wolpert and A. Kolchinsky, Thermodynamics of computing with circuits, *New Journal of Physics* **22**, 063047 (2020).

[18] N. Freitas, J.-C. Delvenne, and M. Esposito, Stochastic thermodynamics of nonlinear electronic circuits: A realistic framework for computing around kt, *Physical Review X* **11**, 031064 (2021).

[19] C. Y. Gao and D. T. Limmer, Principles of low dissipation computing from a stochastic circuit model, *Phys. Rev. Res.* **3**, 033169 (2021).

[20] M. Konopik, T. Korten, E. Lutz, and H. Linke, Fundamental energy cost of finite-time parallelizable computing, *Nature Communications* **14**, 10.1038/s41467-023-36020-2 (2023).

[21] F. Meier, M. Huber, P. Erker, and J. Xuereb, Autonomous quantum processing unit: An autonomous thermal computing machine & its physical limitations (2024).

[22] A. Auffèves, Quantum technologies need a quantum energy initiative, *PRX Quantum* **3**, 020101 (2022).

[23] G. Manzano, G. Kardeş, E. Roldán, and D. H. Wolpert, Thermodynamics of computations with absolute irreversibility, unidirectional transitions, and stochastic computation times, *Phys. Rev. X* **14**, 021026 (2024).

[24] T. Van Vu and K. Saito, Time-cost-error trade-off relation in thermodynamics: The third law and beyond, *Physical Review X* **15**, 10.1103/16b9-rg1j (2025).

[25] A. Bérut, A. Arakelyan, A. Petrosyan, S. Ciliberto, R. Dillenschneider, and E. Lutz, Experimental verification of landauer’s principle linking information and thermodynamics, *Nature* **483**, 187 (2012).

[26] Y. Jun, M. Gavrilov, and J. Bechhoefer, High-precision test of landauer’s principle in a feedback trap, *Phys. Rev. Lett.* **113**, 190601 (2014).

[27] J. Hong, B. Lambson, S. Dhuey, and J. Bokor, Experimental test of landauer’s principle in single-bit operations on nanomagnetic memory bits, *Science Advances* **2**, 10.1126/sciadv.1501492 (2016).

[28] L. Martini, M. Pancaldi, M. Madami, P. Vavassori, G. Gubbiotti, S. Tacchi, F. Hartmann, M. Emmerling, S. Höfling, L. Worschech, and G. Carlotti, Experimental and theoretical analysis of landauer erasure in nanomagnetic switches of different sizes, *Nano Energy* **19**, 108 (2016).

[29] R. Gaudenzi, E. Burzurí, S. Maegawa, H. S. J. van der Zant, and F. Luis, Quantum landauer erasure with a molecular nanomagnet, *Nat. Phys.* **14**, 565 (2018).

[30] M. Scandi, D. Barker, S. Lehmann, K. A. Dick, V. F. Maisi, and M. Perarnau-Llobet, Minimally dissipative information erasure in a quantum dot via thermodynamic length, *Phys. Rev. Lett.* **129**, 270601 (2022).

[31] M. Horowitz, E. Alon, D. Patil, S. Naffziger, R. Kumar, and K. Bernstein, Scaling, power, and the future of cmos, in *IEEE International Electron Devices Meeting, 2005. IEDM Technical Digest.* (IEEE, 2005) pp. 9–15.

[32] M. P. Frank, Introduction to reversible computing: motivation, progress, and challenges, in *Proceedings of the 2nd conference on Computing frontiers*, CF05 (Association for Computing Machinery, New York, NY, USA, 2005) pp. 385–390.

[33] J. Puebla, J. Kim, K. Kondou, and Y. Otani, Spintronic devices for energy-efficient data storage and energy harvesting, *Communications Materials* **1**, 24 (2020).

[34] G. Indiveri and S.-C. Liu, Memory and information processing in neuromorphic systems, *Proceedings of the IEEE* **103**, 1379 (2015).

[35] D. Melanson, M. Abu Khater, M. Aifer, K. Donatella, M. Hunter Gordon, T. Ahle, G. Crooks, A. J. Martinez,

F. Sbahi, and P. J. Coles, Thermodynamic computing system for ai applications, *Nature Communications* **16**, 10.1038/s41467-025-59011-x (2025).

[36] S. Whitelam, Generative thermodynamic computing (2025).

[37] T. Hylton, Thermodynamic neural network, *Entropy* **22**, 256 (2020).

[38] A. B. Boyd, J. P. Crutchfield, M. Gu, and F. C. Binder, Thermodynamic overfitting and generalization: energetics of predictive intelligence, *New Journal of Physics* **27**, 063901 (2025).

[39] H. Zhang, X. Zhang, H. Liu, and Y. Zheng, High-performance near-field radiative thermal logic computing, *Applied Physics Letters* **127**, 10.1063/5.0278815 (2025).

[40] M. Aifer, K. Donatella, M. H. Gordon, S. Duffield, T. Ahle, D. Simpson, G. Crooks, and P. J. Coles, Thermodynamic linear algebra, *npj Unconventional Computing* **1**, 13 (2024).

[41] S. Duffield, M. Aifer, G. Crooks, T. Ahle, and P. J. Coles, Thermodynamic matrix exponentials and thermodynamic parallelism, *Phys. Rev. Res.* **7**, 013147 (2025).

[42] M. Aifer, S. Duffield, K. Donatella, D. Melanson, P. Klett, Z. Belateche, G. Crooks, A. J. Martinez, and P. J. Coles, *Thermodynamic bayesian inference* (2024).

[43] P. Lipka-Bartosik, K. Donatella, M. Aifer, D. Melanson, M. Perarnau-Llobet, N. Brunner, and P. J. Coles, Thermodynamic algorithms for quadratic programming, in *2024 IEEE International Conference on Rebooting Computing (ICRC)* (IEEE, 2024) pp. 1–13.

[44] K. Donatella, S. Duffield, D. Melanson, M. Aifer, P. Klett, R. Salegame, Z. Belateche, G. Crooks, A. J. Martinez, and P. J. Coles, *Scalable thermodynamic second-order optimization* (2025).

[45] E. Aurell, C. Mejía-Monasterio, and P. Muratore-Ginanneschi, Optimal protocols and optimal transport in stochastic thermodynamics, *Phys. Rev. Lett.* **106**, 250601 (2011).

[46] P. Abiuso, V. Holubec, J. Anders, Z. Ye, F. Cerisola, and M. Perarnau-Llobet, Thermodynamics and optimal protocols of multidimensional quadratic brownian systems, *Journal of Physics Communications* **6**, 063001 (2022).

[47] T. Van Vu and K. Saito, Thermodynamic unification of optimal transport: Thermodynamic uncertainty relation, minimum dissipation, and thermodynamic speed limits, *Physical Review X* **13**, 011013 (2023).

[48] S. Whitelam, Increasing the clock speed of a thermodynamic computer by adding noise, *npj Unconventional Computing* **2**, 10.1038/s44335-025-00038-0 (2025).

[49] S. Whitelam and C. Casert, *Thermodynamic computing out of equilibrium* (2024).

[50] A. Dechant and Y. Sakurai, *Thermodynamic interpretation of wasserstein distance* (2019).

[51] M. Nakazato and S. Ito, Geometrical aspects of entropy production in stochastic thermodynamics based on wasserstein distance, *Phys. Rev. Res.* **3**, 043093 (2021).

[52] J. M. Rabaey, A. P. Chandrakasan, and B. Nikolić, *Digital integrated circuits*, 2nd ed., Prentice Hall electronics and VLSI series (Pearson Education, Upper Saddle River, NJ, 2003) includes index. - Previous ed.: 1996.

[53] M. Aifer, S. Duffield, K. Donatella, D. Melanson, P. Klett, Z. Belateche, G. Crooks, A. J. Martinez, and P. J. Coles, *Thermodynamic bayesian inference* (2024).

[54] H. Risken, *The Fokker-Planck Equation* (Springer Berlin Heidelberg, 1996) pp. 63–95.

[55] S. Ciliberto, Experiments in stochastic thermodynamics: Short history and perspectives, *Phys. Rev. X* **7**, 021051 (2017).

[56] D. Gao, W. Ding, M. Nieto-Vesperinas, X. Ding, M. Rahman, T. Zhang, C. Lim, and C.-W. Qiu, Optical manipulation from the microscale to the nanoscale: fundamentals, advances and prospects, *Light: Science & Applications* **6**, 17039 (2017).

[57] K. Sekimoto, Langevin equation and thermodynamics, *Progress of Theoretical Physics Supplement* **130**, 17 (1998), eprint: <https://academic.oup.com/ptps/article-pdf/doi/10.1143/PTPS.130.17/5213518/130-17.pdf>.

[58] U. Seifert, Stochastic thermodynamics, fluctuation theorems and molecular machines, *Reports on Progress in Physics* **75**, 126001 (2012).

[59] C. Villani, *Optimal Transport*, Vol. 338 (Springer Berlin Heidelberg, 2009).

[60] M. Gelbrich, On a formula for the l2 wasserstein metric between measures on euclidean and hilbert spaces, *Mathematische Nachrichten* **147**, 185 (1990).

[61] R. Bhatia, T. Jain, and Y. Lim, On the bures–wasserstein distance between positive definite matrices, *Expositiones Mathematicae* **37**, 165 (2019).

[62] D. A. Sivak and G. E. Crooks, Thermodynamic metrics and optimal paths, *Phys. Rev. Lett.* **108**, 190602 (2012).

[63] V. Cavina, A. Mari, and V. Giovannetti, Slow dynamics and thermodynamics of open quantum systems, *Phys. Rev. Lett.* **119**, 050601 (2017).

[64] P. Abiuso, H. J. D. Miller, M. Perarnau-Llobet, and M. Scandi, Geometric optimisation of quantum thermodynamic processes, *Entropy* **22**, 1076 (2020).

[65] A. Rolandi, M. Perarnau-Llobet, and H. J. D. Miller, Optimal control of dissipation and work fluctuations for rapidly driven systems, *New Journal of Physics* **25**, 073005 (2023).

[66] G. Tsormpatzoglou, F. Sabo, and A. Todri-Sanial, Thermodynamics-inspired computing with oscillatory neural networks for inverse matrix computation (2025).

[67] T. Van Vu and Y. Hasegawa, Geometrical bounds of the irreversibility in markovian systems, *Phys. Rev. Lett.* **126**, 010601 (2021).

[68] P. Lipka-Bartosik, M. Perarnau-Llobet, and N. Brunner, Thermodynamic computing via autonomous quantum thermal machines, *Science Advances* **10**, 10.1126/sci-adv.adm8792 (2024).

[69] I. V. Vovchenko, A. A. Zyablovsky, A. A. Pukhov, and E. S. Andrianov, Thermodynamic coprocessor for linear operations with input-size-independent calculation time based on open quantum system (2025).

[70] J. Hnybida and S. Verret, Minimal-dissipation learning for energy-based models (2025).

[71] I. Bengtsson and K. Zyczkowski, *Geometry of Quantum States: An Introduction to Quantum Entanglement* (Cambridge University Press, 2009).

A. Quadratic Systems

1. Dynamics

We consider a system of N Brownian particles described by the position vector x and interacting using an arbitrary quadratic time-dependent potential $V(x, t)$, that is

$$V(x, t) = \frac{1}{2} x^T K(t) x . \quad (\text{A1})$$

The symmetric and positive semi-definite matrix K describes the interactions between the particles. The systems' dynamics is governed by the potential $V(x, t)$, as well as a random stochastic force η modeled as Gaussian white noise, i.e. $\langle \eta \rangle = 0$ with $\langle \eta_i(t) \eta_j(t') \rangle = \delta_{ij} \delta(t - t')$. As a consequence, we describe the system evolution using a set of overdamped Langevin equations of the form

$$\dot{x} = -\frac{1}{\gamma} \nabla_x V(x, t) + \sqrt{\frac{2}{\gamma \beta}} \eta = -\frac{1}{\gamma} K(t) x + \sqrt{\frac{2}{\gamma \beta}} \eta. \quad (\text{A2})$$

We will assume that the system initially starts in a Gaussian state at time $t = 0$, hence it remains Gaussian at all times $t > 0$. Consequently, its state can and can be described using a probability density function:

$$\rho(x, t) = \frac{1}{\sqrt{(2\pi)^N \det \Sigma(t)}} \exp\left(-\frac{1}{2} x^T \Sigma(t)^{-1} x\right) , \quad (\text{A3})$$

where the covariance matrix $\Sigma(t) = \langle xx^T \rangle(t)$, which provides a full description of the state at time t . It is worth noting that this PDF has zero mean $\langle x \rangle = 0$, however it can be easily generalized to a case where the mean of the distribution is non-trivial. We can obtain a differential equation for the covariance matrix by observing that $\dot{\Sigma} = \langle x \dot{x}^T \rangle + \langle \dot{x} x^T \rangle$ and using [eq. \(A2\)](#)

$$\dot{\Sigma}(t) = -K(t)\Sigma(t) - \Sigma(t)K(t) + \frac{2}{\beta} \mathbf{1} , \quad (\text{A4})$$

where we set $\gamma = 1$. For a given control trajectory $K(t)$ this equation is solved by

$$\Sigma(t) = e^{-\int_0^t ds K(s)} \Sigma(0) e^{-\int_0^t ds K(s)} + \frac{2}{\beta} \int_0^t ds e^{-2 \int_s^t dr K(r)} . \quad (\text{A5})$$

If instead we consider a fixed state trajectory $\Sigma(t)$, we can solve for the control $K(t)$ that realizes that trajectory

$$K(t) = \beta^{-1} \Sigma(t)^{-1} - \int_0^\infty d\nu e^{-\nu \Sigma(t)} \dot{\Sigma}(t) e^{-\nu \Sigma(t)} . \quad (\text{A6})$$

The expressions we obtained here will be used later when we will look for optimal protocols. Moreover, we will refer to $K(t)$ as a finite-time protocol that is realized in some time $\tau > 0$. Given that for $t > \tau$ the control remains constant, we can see from [eq. \(A5\)](#) that the state converges to its thermal state, with covariance matrix $\Sigma_{th} = \beta^{-1} K(\tau)^{-1}$.

2. Thermodynamics

The average internal energy of a system in the potential from [eq. \(A1\)](#) is given by

$$E(t) = \int dx \rho(x, t) V(x, t) = \frac{1}{2} \sum_{i,j} K_{ij}(t) \langle x_i x_j \rangle(t) = \frac{1}{2} \text{Tr}[K(t)\Sigma(t)] . \quad (\text{A7})$$

In stochastic thermodynamics the work \dot{W} and heat \dot{Q} fluxes of the system are traditionally defined as [\[58\]](#):

$$\dot{W}(t) := \frac{1}{2} \text{Tr}[\dot{K}(t)\Sigma(t)] , \quad \dot{Q}(t) := \frac{1}{2} \text{Tr}[K(t)\dot{\Sigma}(t)] . \quad (\text{A8})$$

Integrating the work flux over time and using [eq. \(A6\)](#) we find

$$W = \frac{1}{2} \int_0^\tau dt \text{Tr}[\dot{K}(t)\Sigma(t)] , \quad (\text{A9})$$

$$= \frac{1}{2} \text{Tr}[K(t)\Sigma(t)] \Big|_0^\tau - \frac{1}{2\beta} \ln \det \Sigma(t) \Big|_0^\tau + \frac{1}{2} \int_0^\tau dt \text{Tr} \left[\int_0^\infty d\nu e^{-\nu \Sigma(t)} \dot{\Sigma}(t) e^{-\nu \Sigma(t)} \dot{\Sigma}(t) \right] . \quad (\text{A10})$$

Now let us make two observations. First, note that the quantity

$$\frac{1}{2} \ln \det \Sigma(t) \Big|_0^\tau = - \left[\int dx \rho(x, t) \ln \rho(x, t) \right]_0^\tau = \Delta S \quad (\text{A11})$$

is the change of the von Neumann entropy of the system. Second, observe that the term

$$\frac{1}{2} \text{Tr}[K(t)\Sigma(t)] \Big|_0^\tau = E(\tau) - E(0) = \Delta E, \quad (\text{A12})$$

is the energy change of the system during the protocol. Therefore we can identify the first two terms as the difference in non-equilibrium free energy ($F = E - \beta^{-1}S$). This leads to the last term corresponding to the dissipated work $W_{\text{diss}} := W - \Delta F$

$$W_{\text{diss}} = \frac{1}{2} \int_0^\tau dt \text{Tr} \left[\int_0^\infty e^{-\nu \Sigma(t)} \dot{\Sigma}(t) e^{-\nu \Sigma(t)} \dot{\Sigma}(t) d\nu \right]. \quad (\text{A13})$$

The above integral is precisely the integral over time of a Bures-Wasserstein (BW) quadratic form. More specifically, by defining $\mathcal{BW}(\Sigma, \Sigma + d\Sigma)^2 := g_\Sigma(d\Sigma, d\Sigma)$ with

$$g_\Sigma(A, B) = \frac{1}{2} \int_0^\infty \text{Tr}[e^{-\nu \Sigma} A e^{-\nu \Sigma} B] d\nu, \quad (\text{A14})$$

one can express the entropy production from [eq. \(A13\)](#) as

$$W_{\text{diss}} = \int_0^\tau g_\Sigma(\dot{\Sigma}, \dot{\Sigma}) dt. \quad (\text{A15})$$

Consider now a finite-time protocol with endpoints $\Sigma_0 = \Sigma(0)$ and $\Sigma_1 = \Sigma(\tau)$. For such process we can obtain an achievable lower bound on W_{diss} by computing the geodesic with respect to the Bures-Wasserstein quadratic form. In the current context this is given by

$$W_{\text{diss}} \geq \frac{\mathcal{BW}(\Sigma_0, \Sigma_1)^2}{\tau}, \quad (\text{A16})$$

where \mathcal{BW} is the Bures-Wasserstein distance [\[71\]](#) defined as

$$\mathcal{BW}(\Sigma_0, \Sigma_1)^2 := \text{Tr}[\Sigma_0] + \text{Tr}[\Sigma_1] - 2 \text{Tr} \left[(\Sigma_0^{1/2} \Sigma_1 \Sigma_0^{1/2})^{1/2} \right]. \quad (\text{A17})$$

For our use-case, it is worth noting that we can freely choose $\Sigma_0 \propto \mathbb{1}$, and therefore it is useful to consider [eq. \(A17\)](#) when $[\Sigma_0, \Sigma_1] = 0$. In particular, if we denote by $\sigma_i^{(j)}$ the eigenvalues of Σ_i we find that the distance splits as a sum over the eigenvalues of the matrices

$$\mathcal{BW}(\Sigma_0, \Sigma_1)^2 = \sum_{\alpha} (\sqrt{\sigma_{0,\alpha}} - \sqrt{\sigma_{1,\alpha}})^2. \quad (\text{A18})$$

B. Symmetries in Driving Protocols

The design of EDP-optimal driving protocols can be simplified by using two complementary symmetries of the entropy production W_{diss} , namely temperature rescaling which increases linearly the entropy production, and time-strength rescaling which leaves the EDP invariant.

Temperature rescaling. From the evolution equation for the covariance matrix $\Sigma(t)$ ([eq. \(A5\)](#)) one sees that $\Sigma(t) \propto \beta^{-1}$ (since the initial state is a thermal distribution). Therefore, the transformation $\beta^{-1} \rightarrow \lambda \beta^{-1}$ leads to

$$\Sigma(t) \rightarrow \lambda \Sigma(t), \quad \dot{\Sigma}(t) \rightarrow \lambda \dot{\Sigma}(t), \quad (\text{B1})$$

which, upon substitution into the definition of irreversible work ([eq. \(23\)](#)), yields

$$W_{\text{diss}} \rightarrow \frac{\lambda^2}{2} \int_0^\tau dt \text{Tr} \left[\int_0^\infty d\nu e^{-\nu \lambda \Sigma(t)} \dot{\Sigma}(t) e^{-\nu \lambda \Sigma(t)} \dot{\Sigma}(t) \right] = \lambda W_{\text{diss}}, \quad (\text{B2})$$

where we used a change in variable on ν . Thus, W_{diss} is *linear* in the temperature β^{-1} .

Time-strength rescaling. Consider a finite-time protocol $K(t)$ over $t \in [0, \tau]$. The transformation

$$K(t) \longrightarrow K'(t) = \lambda K(\lambda t), \quad t \in [0, \tau/\lambda], \quad (\text{B3})$$

simultaneously amplifies the control strength by λ and compresses its duration to τ/λ . One then finds that the new covariance $\Sigma'(t)$ evolves as

$$\Sigma'(t) = e^{-\int_0^t ds \lambda K(\lambda s)} \lambda^{-1} \Sigma(0) e^{-\int_0^t ds \lambda K(\lambda s)} + \frac{2}{\beta} \int_0^t ds e^{-2 \int_s^t dr \lambda K(\lambda r)} = \lambda^{-1} \Sigma(\lambda t). \quad (\text{B4})$$

This leads to the following rescaling

$$\Sigma(t) \longrightarrow \lambda^{-1} \Sigma(\lambda t), \quad \dot{\Sigma}(t) \longrightarrow \dot{\Sigma}(\lambda t). \quad (\text{B5})$$

Substituting this into [eq. \(23\)](#) shows

$$W_{\text{diss}} \longrightarrow \frac{1}{2} \int_0^{\tau/\lambda} dt \text{Tr} \left[\int_0^\infty d\nu e^{-\nu \lambda^{-1} \Sigma(\lambda t)} \dot{\Sigma}(\lambda t) e^{-\nu \lambda^{-1} \Sigma(\lambda t)} \dot{\Sigma}(\lambda t) \right] = W_{\text{diss}}, \quad (\text{B6})$$

so W_{diss} is invariant under the action from [eq. \(B3\)](#). This symmetry implies that amplifying the protocol's strength by λ while compressing its duration to τ/λ yields an equivalent thermodynamic outcome. Formally, the transformations form the Lie group (\mathbb{R}^+, \cdot) , acting on the space of protocols \mathcal{F} . The orbit of a protocol $K(t)$, given by $\{\lambda K(\lambda t) \mid \lambda \in \mathbb{R}^+\}$, defines an equivalence class with constant EDP. This scaling symmetry reduces the optimization problem by allowing us to search for optimal protocols within the quotient space \mathcal{F}/\mathbb{R}^+ .

Implications for optimization. The time-strength symmetry $K(t) \rightarrow \lambda K(\lambda t)$ partitions the space of protocols \mathcal{F} into orbits (equivalence classes) of constant irreversible work. Hence one can restrict the search for EDP-optimal protocols to the quotient space \mathcal{F}/\mathbb{R}^+ . Finally, both of the discussed symmetries for entropy production also hold for the Bures-Wasserstein distance, as it is realized by the geodesic protocol.

C. Further Details of Protocols

1. Quenches and Bang-Bang Protocols

In a quench protocol (see Ref. [40]) the system potential is driven instantaneously from $V_0(x)$ to $V_1(x)$, meaning that formally $\tau_D = 0$. The process can therefore be written as

$$(\Sigma_0, K_0) \xrightarrow[(a)]{\text{quench}} (\Sigma_0, K_1) \xrightarrow[(b)]{\text{thermalization}} (\Sigma_1, K_1). \quad (\text{C1})$$

In sub-process (a) we have:

$$W_a = \frac{1}{2} \text{tr}[(K_1 - K_0)\Sigma_0], \quad \Delta E_a = \frac{1}{2} \text{Tr}[(K_1 - K_0)\Sigma_0], \quad \Delta S_a = 0. \quad (\text{C2})$$

In sub-process (b) we have:

$$W_b = 0, \quad \Delta E_b = \frac{1}{2} \text{Tr}[K_1(\Sigma_1 - \Sigma_0)], \quad \Delta S_b = \frac{1}{2}(\ln \det \Sigma_1 - \ln \det \Sigma_0). \quad (\text{C3})$$

Therefore the entropy production during the whole protocol composed of steps (a) and (b) is given by

$$W_{\text{diss}}^Q = \sum_{x \in \{a,b\}} W_x - (\Delta E_x - T\Delta S_x) = \frac{1}{2} \text{Tr}[K_1(\Sigma_0 - \Sigma_1)] + \frac{1}{2} T \ln \left(\frac{\det \Sigma_1}{\det \Sigma_0} \right), \quad (\text{C4})$$

then we simply take Σ_0 and Σ_1 to be their respective thermal states.

Using this same approach we can consider Bang-Bang protocols, where a quench is performed to an intermediary control K_* at $t = 0$ and a second quench to K_1 is performed at $t = \tau_D/2$

$$W_{\text{diss}}^{\text{Bang-Bang}} = W_{\text{diss}}^Q - \frac{1}{2} \text{Tr}[(K_1 - K_*)(T K_0^{-1} - \Sigma_*)], \quad (\text{C5})$$

where we can compute Σ_* with [eq. \(A5\)](#)

$$\Sigma_* = e^{-K_* \tau_D/2} \Sigma_0 e^{-K_* \tau_D/2} + (\mathbb{1} - e^{-K_* \tau_D}) T K_*^{-1}. \quad (\text{C6})$$

2. Geodesics

Generally, all protocols will dissipate some energy into the environment. It can be shown that for the system at hand, we can describe it as a property of the length of a trajectory in the state space equipped with the Bures-Wasserstein metric [46]. This implies that we can minimize it with a protocol that matches geodesics in this space

$$\Sigma_{\text{geo}}(t) = (1-s)^2 \Sigma_0 + s^2 \Sigma_1 + s(1-s)(\sqrt{\Sigma_0 \Sigma_1} + \sqrt{\Sigma_1 \Sigma_0}) \quad (\text{C7})$$

where $s = t/\tau_D$. The state, the corresponding control that realizes it is obtained by inserting the geodesic state trajectory into [eq. \(A6\)](#)

$$K(t) = T \Sigma_{\text{geo}}(t)^{-1} - \frac{1}{\tau_D} \left(s \Sigma_1 + (1-2s) \sqrt{T \Sigma_1} - (1-s) T \mathbb{1} \right) \Sigma_{\text{geo}}(t)^{-1}, \quad (\text{C8})$$

for $0 < t < \tau_D$. It is worth noting that since at the extremities of the protocol we have $K(0) = T \Sigma_0^{-1}$ and $K(\tau) = T \Sigma_1^{-1}$ [eq. \(C8\)](#) implies that there will be jumps at the beginning and end of the protocol:

$$K(0^+) - K(0) = \frac{1}{\tau} \left(\mathbb{1} - \sqrt{\Sigma_1 / \Sigma_0} \right), \quad (\text{C9})$$

$$K(\tau) - K(\tau^-) = \frac{1}{\tau} \left(\mathbb{1} - \sqrt{\Sigma_0 / \Sigma_1} \right). \quad (\text{C10})$$

This protocol will dissipate

$$W_{\text{diss}}^{(\text{opt})} = \frac{\mathcal{BW}(\Sigma_0, \Sigma_1)^2}{\tau_D}. \quad (\text{C11})$$

3. Slow driving protocols

The metric featured in [eq. \(A15\)](#) is dependent on the state of the system (encoded in $\Sigma(t)$) instead of the externally-controlled $K(t)$. This implies that for a given protocol on the system, the dissipated work depends on the exact solution of the dynamics [\(A4\)](#). However, in the slow driving limit [46] (at first order) this dependence greatly simplifies. In this limit we only consider the control over the trajectory. We can simplify the analysis of comparing different protocols by restricting ourselves to the slow-driving regime and expanding [eq. \(A15\)](#) via $\Sigma(t) = K^{-1}(t) + \mathcal{O}(\tau^{-1})$, as

$$W_{\text{diss}} = \int_0^\tau g_{K^{-1}}(K^{-1} \dot{K} K^{-1}, K^{-1} \dot{K} K^{-1}) dt + \mathcal{O}(\tau^{-2}) \quad (\text{C12})$$

This expression further simplifies in the commuting case $[K_1, K_0] = 0$,

$$W_{\text{diss}} = \frac{1}{4} \int_0^\tau \text{Tr} \left[\frac{\dot{K}(t)^2}{K(t)^3} \right] + \mathcal{O}(\tau^{-2}), \quad (\text{C13})$$

or equivalently with the eigenvalues of K

$$W_{\text{diss}} = \frac{1}{4} \int_0^\tau dt \sum_i \frac{\dot{\kappa}_i^2}{\kappa_i^3}. \quad (\text{C14})$$

If we decompose the boundary conditions in terms of their eigenvalue $k^{(i)}$ we obtain

$$W_{\text{diss}} = \sum_i f(k_i^{(0)}, k_i^{(1)}), \quad (\text{C15})$$

with $f(x, y) = \frac{T(x-y)^2}{4} \int_0^\tau dt \frac{\dot{s}(t)^2}{((1-s(t))x + s(t)y)^3}$. If the matrices K_0 and K_1 are sampled from some distribution, the average $\langle W_{\text{diss}} \rangle$, as well as its fluctuations, will depend on it. Here let us make us two observations. Assume for simplicity that $K_0 \propto \mathbb{1}$, therefore $k_i^{(0)} \equiv \bar{\kappa}$. We have

$$\langle W_{\text{diss}} \rangle = \sum_i \langle f(\bar{\kappa}, k_i^{(1)}) \rangle \quad (\text{C16})$$

When the sample distribution of K_1 is isotropic, then we expect the eigenvalues to be identically distributed. Which implies that the expectation value of the dissipation is given by

$$N\langle f(\bar{\kappa}, k_1) \rangle. \quad (\text{C17})$$

In general we do not have explicit versions of $f(x, y)$, however for some cases it is simple enough that we can use the expression to compute expectation values. For example, in the case of a linear ramp we have $f(x, y) = \frac{T(x-y)^2(x+y)}{8x^2y^2}$. Secondly, if the eigenvalues k_i are also uncorrelated, we will have

$$\text{Var}(W_{\text{diss}}) = N\text{Var}(f(\bar{\kappa}, k_1)) \quad (\text{C18})$$

which explains the concentration of W_{diss} for large N . Notice that the same happens whenever the eigenvalues k_i are not "fully correlated", i.e. whenever $\text{Var}[\sum_i f(\bar{\kappa}, k_i)] = \mathcal{O}(N^\alpha)$ with $\alpha < 2$.

D. Natural squeezing and partial optimization of $W_{\text{diss}}^{(\text{opt})}$

Consider the standard case in which either the initial or the final covariance matrix (and associated quadratic potential) is isotropic, e.g. boundary conditions of the form

$$\Sigma_0 = \alpha \mathbb{1}, \quad \Sigma_1 = K^{-1}, \quad (\text{D1})$$

to which is associated a minimum dissipation given by the \mathcal{BW} distance (A17)-(A18)

$$\mathcal{BW}^2 = \text{Tr}[(\sqrt{\alpha} \mathbb{1} - K^{-1/2})^2]. \quad (\text{D2})$$

Assuming, e.g., that the initial (idle-mode) squeezing α^{-1} is under experimental control, we will now provide useful bounds to the minimization of \mathcal{BW} . Similar considerations follow when the squeezing of K can be tuned.

1. Tuning α

When being able to tune α , the minimum of the quadratic expression (D2) is obtained for α^* satisfying

$$N\sqrt{\alpha^*} = \text{Tr}[K^{-1/2}], \quad (\text{D3})$$

N being the dimension of the matrices we are considering. Clearly we cannot, in general, assume to know $\text{Tr}[K^{-1/2}]$, as this would need diagonalizing/inverting the matrix K . We can however provide lower bounds which then serve as a rule of thumb for choosing α .

For example from the mean-inequalities we know that for positive eigenvalues λ_i it holds

$$\left(\frac{1}{N} \sum_i \lambda_i^{-1/2}\right)^{-2} \leq \left(\prod_i \lambda_i\right)^{\frac{1}{N}} \leq \frac{1}{N} \sum_i \lambda_i. \quad (\text{D4})$$

The same inequality can thus be re-expressed as

$$\alpha^* \geq (\det K)^{-\frac{1}{N}} \geq \frac{N}{\text{Tr}[K]}. \quad (\text{D5})$$

Notice that it is only possible to *lower* bound α^* without using "expensive" calculations, as there could always be eigenvalues of K small enough to make the optimal α^* increase. However, if we include semi-definite-programming (SDPs) in the set of functions that are "not expensive" to compute, we can access to λ_{\min} of K and bound

$$\alpha^* \leq \frac{1}{\lambda_{\min}}. \quad (\text{D6})$$

2. Fixed α , rescaling K

Suppose now that α is fixed, but we have the freedom to rescale K (this corresponds to a case in which one does not have experimental control over the squeezing of the idle-mode of the thermodynamics machine, but is free to remap the problem of interest by rescaling the coordinates of $\rho(x)$). We thus consider

$$\mathcal{BW}^2 = \text{Tr}[(\sqrt{\alpha} \mathbb{1} - \eta^{-1/2} K^{-1/2})^2] \quad (\text{D7})$$

and vary η . One can easily see that the minimum is obtained for

$$\sqrt{\alpha} \operatorname{Tr}[K^{-1/2}] = \eta^{*-1/2} \operatorname{Tr}[K^{-1}] . \quad (\text{D8})$$

Once again, one can use inequalities to give bounds to η^* . For example noticing

$$\frac{\operatorname{Tr}[K^{-1}]}{\operatorname{Tr}[K^{-1/2}]} \leq \lambda_{\min}^{-1/2} , \quad (\text{D9})$$

one gets

$$\eta^* \leq \frac{\lambda_{\min}^{-1}}{\alpha} . \quad (\text{D10})$$

Similarly, via a Cauchy-Schwarz inequality we have

$$\frac{\operatorname{Tr}[K^{-1}]}{\operatorname{Tr}[K^{-1/2}]} \geq \frac{\operatorname{Tr}[K^{-1/2}]}{N} \geq \frac{\sqrt{N}}{\sqrt{\operatorname{Tr}[K]}} , \quad (\text{D11})$$

and therefore

$$\eta^* \geq \frac{N}{\alpha \operatorname{Tr}[K]} . \quad (\text{D12})$$

Notice that these inequalities obtained for η^* are dual to those for α^* above.